Improved Biquad Structures Using Double-Output Transconductance Blocks for Tunable Continuous-Time Filters

VLADIMIR I. PRODANOV AND MICHAEL M. GREEN

Department of Electrical Engineering, University at Stony Brook, Stony Brook, NY 11794-2350

Abstract. A family of $g_m - C$ biquad structures is derived. These biquads require only a pair of grounded capacitors and three transconductors. It is shown that a pair of complex zeros can be realized simply by replicating the output stage of the transconductance block, thereby constructing a second output current that is proportional to the original output current. Although these biquad structures are very compact, they allow independent programming of the filter's center frequency and Q. IC simulations and measurements are presented using a fifth-order tunable filter as an example.

Key Words: active filters, biquadratic filters, continous-time filters, tunable filters, analog integrated circuits

1. Introduction

In general there are two analog filter synthesis techniques: the passive prototype-based technique and the biquad-based technique. Biquads are preferred when the desired filter transfer function has finite zeros. In the last decade many different $g_m - C$ biquad structures for monolithic filter implementation have been reported [2], [5], [1]. These biquads are all based on realizing a pair of poles using a set of integrators connected with feedback; the transmission zeros are then obtained by injecting weighted signals into the loop. As discussed in [5], there are two ways of achieving these zeros without disturbing the location of the two poles:

1. By coupling the input voltage to an appropriate node (or set of nodes). In many cases this procedure results in a structure that contains floating capacitors and hence requires input buffering.
2. By feeding additional current (generated using an additional transconductor) into a node with some fixed impedance connected to ground. Using this approach one can design highly flexible biquads ([1], [4]) that use only grounded capacitors and hence do not require input buffering. Unfortunately, such biquads employ many (7–8) transconductance blocks, which can dissipate excessive power and require large chip area.

In the next section we present two biquad structures which employ only three transconductors and two grounded capacitors, hence conserving both power dissipation and chip area. In Section 3 we discuss the effect of the transconductance block nonidealities on the performance. In Section 4 we give measured results of a fifth-order filter that was designed using these biquad structures.

2. Derivation of the Biquad Structures

Consider the simple structure shown in Fig. 1. The transfer functions V_1/V_{in} and V_2/V_{in} are given by:

$$\frac{V_1}{V_{in}} = \frac{1 + s\frac{C_2}{g_{m2}}}{1 + s\frac{C_1}{g_{m1}} + s^2\frac{C_1C_2}{g_{m1}g_{m2}}} \tag{1}$$

$$\frac{V_2}{V_{in}} = \frac{1}{1 + s\frac{C_1}{g_{m1}} + s^2\frac{C_1C_2}{g_{m1}g_{m2}}} \tag{2}$$

The poles of this circuit are thus given by:

$$s = \frac{g_{m2}}{2C_2}\left(-1 \pm \sqrt{1 - 4\frac{g_{m1}}{g_{m2}}\frac{C_2}{C_1}}\right) \tag{3}$$

A pair of *zeros* can be realized by adding an extra feedforward path; this can be done conveniently by simply adding an extra proportional output to each transconductance block, as shown in Fig. 2.

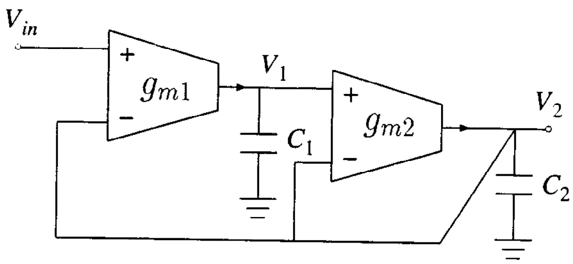

Fig. 1. $g_m - C$ lowpass structure.

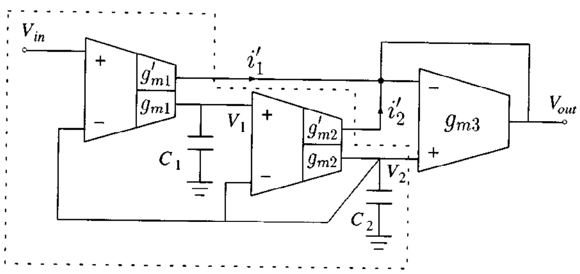

Fig. 2. $g_m - C$ biquad structure that realizes a pair of transmission zeros.

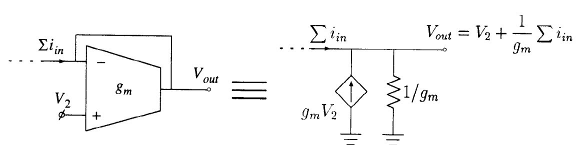

Fig. 3. Using a single-output transconductor as a summer: the circuit and its small signal equivalent.

The core of the Fig. 2 biquad, shown within the dotted lines, is simply the lowpass structure given in Fig. 1. The second outputs (labeled g'_{m1} and g'_{m2}—these will be explained shortly), along with transconductance block g_{m3}, are used to realize the zeros by summing currents i'_1 and i'_2, converting them into a voltage and adding this voltage to V_2. These operations are illustrated in Fig. 3.

To derive the transfer function of this biquad we can write, using Fig. 3,

$$V_{out} = V_2 + \frac{1}{g_{m3}}(i'_1 + i'_2) \tag{4}$$

which gives:

$$V_{out} = V_2 + \frac{1}{g_{m3}}[g'_{m1}(V_{in} - V_2) + g'_{m2}(V_1 - V_2)] \tag{5}$$

Incorporating (1) and (2) into (5), we have the following filter transfer function:

$$\frac{V_{out}}{V_{in}} = \frac{1 + s\left(\frac{1}{k_1}\frac{C_1}{g_{m3}} + \frac{1}{k_2}\frac{C_2}{g_{m3}}\right) + s^2 \frac{C_1 C_2}{k_1 g_{m3} g_{m2}}}{1 + s\frac{C_1}{g_{m1}} + s^2 \frac{C_1 C_2}{g_{m1} g_{m2}}} \tag{6}$$

where $ki_1 \equiv g_{mi}/g'_{mi}$, $i = 1, 2$.

The double-output transconductance blocks shown in Fig. 2 are realized by an additional output stage as illustrated in Fig. 4. Fig. 4(a) shows a conventional single-output transconductor. Fig. 4(b) shows a double-output transconductor with g_m and g'_m of the same sign; notice that the ratio $g_m/g'_m = \frac{(W/L)}{(W/L)'}$. Fig. 4(c) shows a double-output transconductor with g_m and g'_m of opposite sign which is a result of changing the diode connection from transistor M_1 in Fig. 4(b) to transistor M_2 and moving output current i'_{out} to the drain of M_1.

From the transfer function given in (6) we can derive the ω_0 and Q of the quadratic function in the numerator and the denominator:

For the denominator,

$$\omega_{0d} = \sqrt{\frac{g_{m1} g_{m2}}{C_1 C_2}} \;\; Q_d = \sqrt{\frac{g_{m1}}{g_{m2}}\frac{C_2}{C_1}} \tag{7}$$

For the numerator,

$$\omega_{0n} = \sqrt{k_1 \frac{g_{m3} g_{m2}}{C_1 C_2}} \;\; Q_n = \frac{\sqrt{k_1 \frac{g_{m3}}{g_{m2}}\frac{C_2}{C_1}}}{1 + \frac{k_1}{k_2}\frac{C_2}{C_1}} \tag{8}$$

Note that if k_2 is controlled independently from the other transconductances (by varying g'_{m2}), Q_n can be varied while keeping ω_{0n} fixed.

By interchanging the identity of the input and output terminals of the Fig. 2 biquad, as shown in Fig. 5, it is straightforward to show that (1), (2) and (5) will still hold, but with V_{in} and V_{out} interchanged. Thus the transfer function of the Fig. 5 circuit will be the reciprocal of the transfer function given in (6). In this filter, the center frequency and filter Q (determined by the poles) will be given by (8).

Since in the Fig. 5 structure the core two-integrator loop formed by g_{m1}, g_{m2}, C_1 and C_2 determines the *zeros* of its transfer function, it is convenient to break this feedback in the various ways shown in Fig. 6 to realize the following different types of transfer functions:

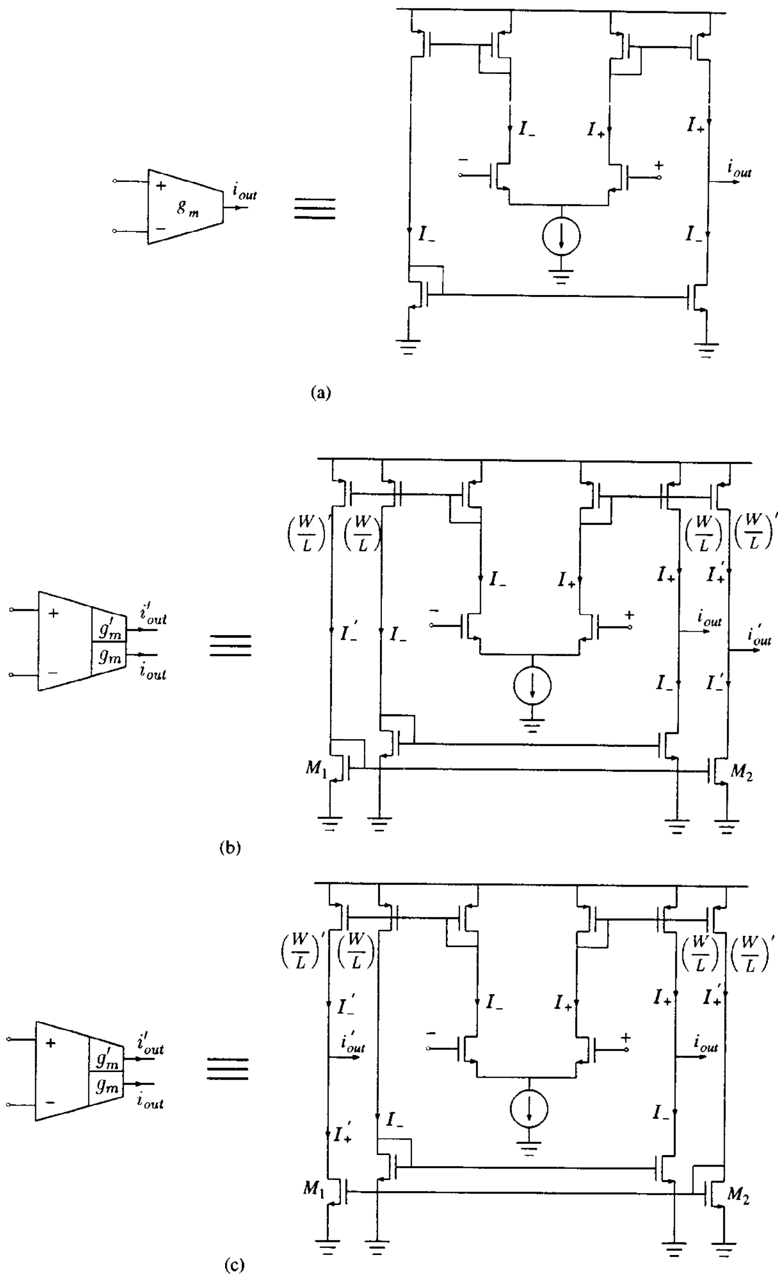

Fig. 4. (a) Single-output transconductor; (b) and (c) Double-output transconductors.

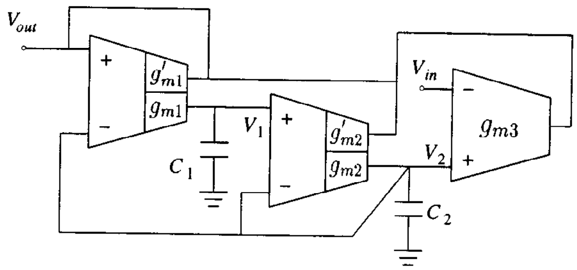

Fig. 5. $g_m - C$ biquad structure reciprocal to the one in Fig. 2.

Fig. 6(a):

$$\frac{V_{out}}{V_{in}} = \frac{s\frac{C_1}{g_{m1}}\left(1+s\frac{C_2}{g_{m2}}\right)}{1+s\left(\frac{1}{k_1}\frac{C_1}{g_{m3}}+\frac{1}{k_2}\frac{C_2}{g_{m3}}\right)+s^2\frac{C_1C_2}{k_1g_{m2}g_{m3}}} \tag{9}$$

Fig. 6(b):

$$\textbf{Notch} \;:\; \frac{V_{out}}{V_{in}} = \frac{1+s^2\frac{C_1C_2}{g_{m1}g_{m2}}}{1+s\frac{C_2}{k_2g_{m3}}+s^2\frac{C_1C_2}{k_1g_{m2}g_{m3}}} \tag{10}$$

$$\textbf{BP} \;:\; \frac{V_1}{V_{in}} = \frac{s\frac{C_2}{g_{m2}}}{1+s\frac{C_2}{k_2g_{m3}}+s^2\frac{C_1C_2}{k_1g_{m2}g_{m3}}} \tag{11}$$

$$\textbf{LP} \;:\; \frac{V_2}{V_{in}} = \frac{1}{1+s\frac{C_2}{k_2g_{m3}}+s^2\frac{C_1C_2}{k_1g_{m2}g_{m3}}} \tag{12}$$

Fig. 6(c):

$$\textbf{HP} \;:\; \frac{V_{out}}{V_{in}} = \frac{s^2\frac{C_1C_2}{g_{m1}g_{m2}}}{1+s\frac{C_2}{k_2g_{m3}}+s^2\frac{C_1C_2}{k_1g_{m2}g_{m3}}} \tag{13}$$

$$\textbf{BP} \;:\; \frac{V_1}{V_{in}} = \frac{s\frac{C_2}{g_{m2}}}{1+s\frac{C_2}{k_2g_{m3}}+s^2\frac{C_1C_2}{k_1g_{m2}g_{m3}}} \tag{14}$$

$$\textbf{LP} \;:\; \frac{V_2}{V_{in}} = \frac{1}{1+s\frac{C_2}{k_2g_{m3}}+s^2\frac{C_1C_2}{k_1g_{m2}g_{m3}}} \tag{15}$$

Notice that the structure in Fig. 6(c) realizes a high pass filter whose loss at low frequencies neither depends on subtraction of signal currents nor requires the use of a floating capacitor. Another $g_m - C$ topology with this same desirable property was first reported in [5].

A further simplification of the biquads presented here is possible. Due to the way the two basic structures are implemented (see equation (4)), the currents I'_{1+}, I'_{1-}, I'_{2+} and I'_{2-} can be directly injected into the output stage of the third transconductor (e.g. Fig. 7) without the need for extra current mirrors, thereby making transistors M_1 and M_2 in the double-output structure (Fig. 4(b) and 4(c)) unnecessary. Hence, we conclude that only *two* transistors must be added to a single-output transconductor to create a double-output transconductor suitable for implementation of the proposed biquad structures, thus further simplifying the circuitry and reducing the output noise.

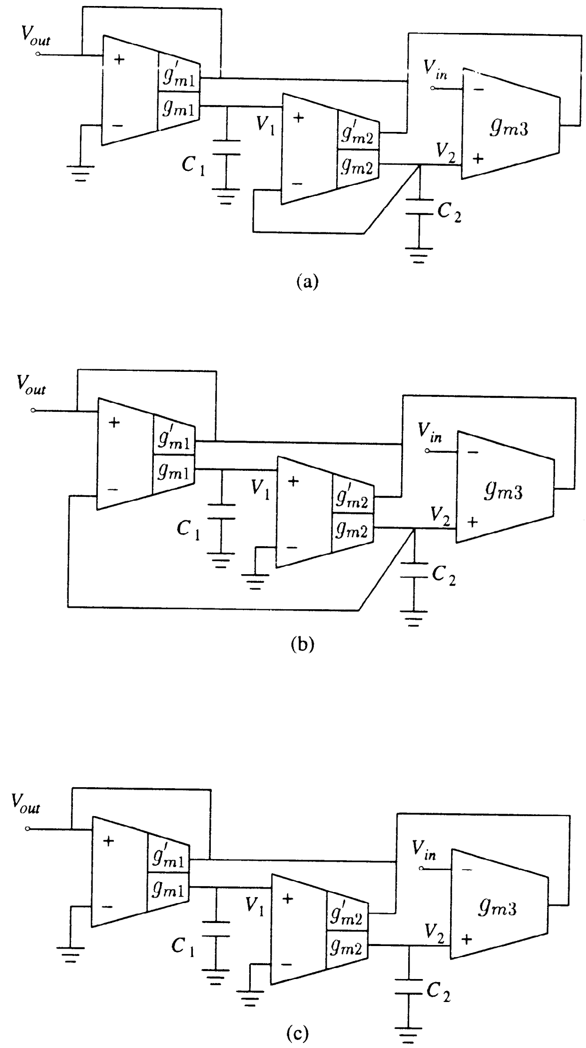

Fig. 6. Additional structures derived by breaking a feedback loop in Fig. 5 circuit.

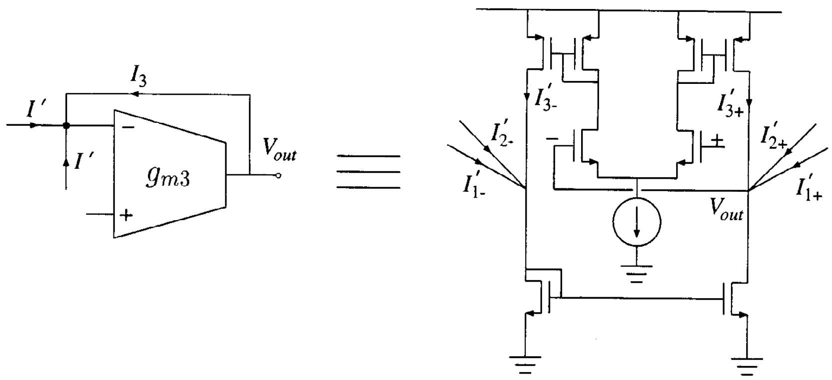

Fig. 7. Avoiding the use of additional current mirrors in the double-output transconductors.

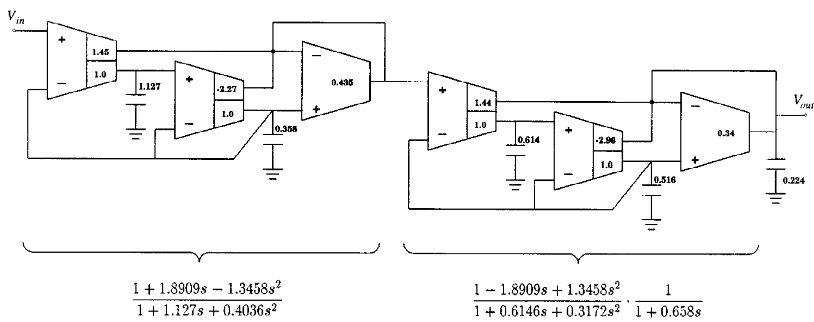

Fig. 8. Block diagram of inverse Gaussian filter.

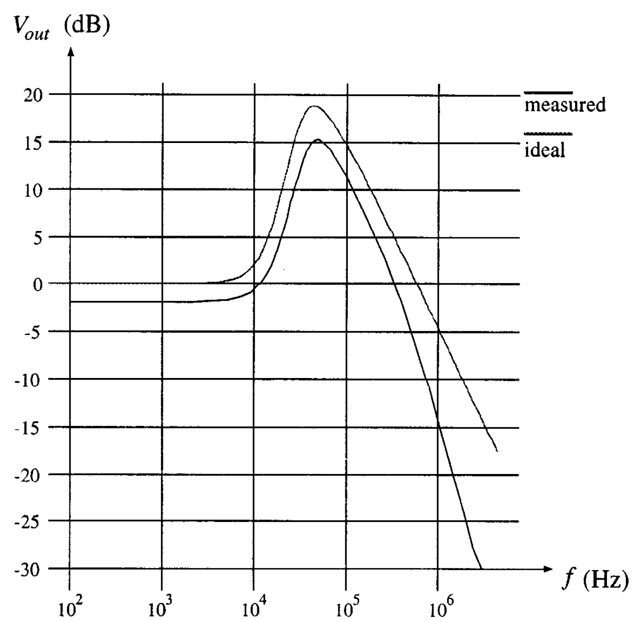

Fig. 9. Ideal and measured magnitude frequency response of filter.

Table 1. Transfer function magnitudes at zero frequency.

Circuit		Low Freq. Transfer Function
Fig. 5		$\frac{V_{out}}{V_{in}}(0) \approx 1 + \frac{g'_{m2}}{g_{m2}}\delta_2 + \left(\frac{g'_{m1}}{g_{m3}} - 1\right)\delta_1$
Fig. 6(a)		$\frac{V_{out}}{V_{in}}(0) \approx \delta_1$
Fig. 6(b)	Notch	$\frac{V_{out}}{V_{in}}(0) \approx 1 - \frac{g'_{m2}}{g_{m3}}\delta_2$
	BP	$\frac{V_1}{V_{in}}(0) \approx \delta_2$
	LP	$\frac{V_2}{V_{in}}(0) \approx 1 - \frac{g'_{m2}}{g_{m3}}\delta_2$
Fig. 6(c)	HP	$\frac{V_{out}}{V_{in}}(0) \approx \delta_1\delta_2$
	BP	$\frac{V_1}{V_{in}}(0) \approx \delta_2$
	LP	$\frac{V_2}{V_{in}}(0) \approx 1 - \frac{g'_{m2}}{g_{m3}}\delta_2$

3. Effect of Nonidealities on the Performance of the Proposed Structures

Some of the factors limiting the performance of the proposed structures, and that of any $g_m - C$ filter in general, are the parameters of the individual transconductance blocks, including: (A) nonzero output admittance; (B) nonzero input admittance; and (C) phase error due to nondominant poles. We will give some results concerning the effect of each of these nonidealities.

A. Nonzero Output Admittance:
The most significant effect of the nonzero output conductance of the transconductance blocks is on the low frequency behavior of the biquads, since most of the transconductance blocks have a capacitor connected to the output. In order to analyze the effect of the nonzero output conductances on the low frequency behavior, the substitution $sC_i \rightarrow g_{oi}$ can be made in each of the transfer functions given in the previous section. A listing of the magnitude, in terms of the of each of the $\delta_i \equiv g_{oi}/g_{mi}$ (i.e., $1/\delta_i$ is the intrinsic gain of the ith transconductance block), of these transfer functions at $s = 0$ is given in Table 1. We assumed that $\delta_i \ll 1$ in order to simplify these expressions.

We now consider the effect of output *capacitance* at each transconductance block. Notice that in all circuits in Fig. 2, Fig. 5 and Fig. 6, there is already a capacitor connected at nodes V_1 and V_2. Hence any additional parasitic capacitance present at these nodes from the transconductance block outputs will only shift the poles and zeros slightly. On the other hand, any capacitance C_3 connected to the output of g_{m3} will contribute a parasitic pole at $s = -g_{m3}/C_3$. However, it can be shown that the *desired* poles and zeros of the Fig. 2 circuit are *not* affected by the presence of this nonzero output capacitance. Unfortunately, this property is not shared by the Fig. 5 and Fig. 6 biquads.

B. Nonzero Input Admittance:
All of the biquads discussed in the previous section (with the exception of the highpass and notch filters) should give a magnitude that approaches zero for sufficiently high frequency. However, if the capacitances that appear across the input terminals of the transconductance blocks are taken into account, then a number of capacitive loops are formed, giving rise to capacitive coupling between the outputs and input. This results in the injection of the input signal into the output nodes at high frequencies, thus creating additional zeros in the transfer functions. As a consequence of these zeros, flattening will be observed at higher frequencies. (As discussed next, however, the transconductance blocks contribute a set of nondominant poles; hence, this flattening will be observed only over a finite range of frequencies.)

C. Nondominant Poles:
All transconductance blocks contribute extra poles due to internal parasitic capacitances. It is discussed in [3] and [6] that in $g_m - C$ filters, the small phase shift that these extra poles contribute can result in a large error in the overall transfer function. However, since the biquads presented here consist of only three transconductance blocks, this error is kept at a minimum.

4. Measured Results

A fifth-order band-limited inverse Gaussian filter using the biquad structure in Fig. 2 was designed and fabricated using the MOSIS $2 - \mu$ Orbit Analog Process. The normalized transfer function of the filter, whose block diagram is shown in Fig. 8 is given by:

$$H(s) = \frac{968.38 - 854.03s^2 + 1752.25s^4}{945 + 2268s + 2419.2s^2 + 1451.5s^3 + 497.7s^4 + 79.6s^5} \qquad (16)$$

The poles and zeros are arranged in such a way that in the normalized frequency range $\omega = 0 - 1.15$ its amplitude response provides equiripple approximation of an inverse Gaussian while having linear (Bassel–Thompson) phase response. This transfer function can be implemented using either two biquad structures and a lossy integrator or two Fig. 2 biquads, one of which is loaded with a capacitor as shown in Fig. 8. Fig. 9 shows both the ideal (taken directly from (16, with appropriate frequency scaling) and measured magnitude frequency response. The effect of the nonidealities discussed in the previous section are evident here. The additional loss in the measured response comes from the nonzero output conductance of the transconductance blocks. The measured rolloff at high frequencies in the measured response is less than the ideal response due to the capacitive coupling of the input capacitance of the transconductance blocks.

5. Conclusion

The derivation of $g_m - C$ biquad topologies which use two output transconductors has been presented. It has been shown that these biquads retain many of the advantages of biquads, including flexibility in specifying various filter parameters, while allowing a very compact design. Measured results showing the performance of a 5-th order monolithic inverse Gaussian filter based on the proposed topology were included.

References

1. C.-M. Chang and P.-C. Chen, "Universal active filter with current gain using OTAs." *International Journal of Electronics* 71(5), pp. 805–808, Nov. 1991.

2. R. L. Geiger and E. Sánchez-Sinencio, "Active filter design using operational transconductance amplifiers; a tutorial." *IEEE Circuit and Devices Mag.* 1, pp. 20–32, March 1985.

3. H. Khorramabadi and P. R. Gray, "High-frequency CMOS continuous-time filters." *IEEE Journal of Solid-State Circuits* 19, pp. 939–948, Dec. 1984.

4. R. Nawrocki and U. Klein, "New OTA-capacitor realization of a universal biquad." *Electronics Letters* 22(1), pp. 50–51, Jan. 1986.

5. E. Sanchez-Sinencio, R. L. Geiger and H. Nevarez-Lozano, "Generation of continuous-time two integrator loop OTA filter structures." *IEEE Transactions on Circuits and Systems* 35(8), pp. 936–945, Aug. 1988.

6. Y.-T. Wang and A. A. Abidi, "CMOS active filter design at very high frequencies." *IEEE Journal of Solid-State Circuits* 25, pp. 1562–1574, Dec. 1990.

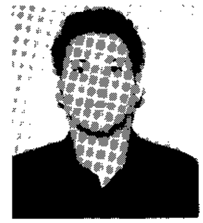

Vladimir I. Prodanov was born in Sofia, Bulgaria on February 3, 1970. He received engineering degree (B.S.) from Technical University, Sofia, Bulgaria in 1991 and M.S. in electrical engineering in 1994 from State University of New York, Stony Brook, USA where he is currently working towards his Ph.D. His research interests include analog (continuous-time) integrated circuits with low supply voltage emphasis.

Michael M. Green received the B.S. degree in electrical engineering from University of California, Berkeley in 1984 and his M.S. and Ph.D. degrees in electrical engineering from University of California, Los Angeles in 1988 and 1991, respectively.

From 1984 to 1987 he was a design engineer in National Semiconductor's audio integrated circuit design group. He is currently an associate professor of electrical engineering at the University of California, Irvine. His research interests include nonlinear circuit theory, analog integrated circuit design and analog circuit simulation.

Dr. Green is a member of Eta Kappa Nu, Tau Beta Pi, and Sigma Xi. From 1992–1994 he was an Associate Editor of the IEEE TRANSACTIONS ON CIRCUITS AND SYSTEMS—I and of the IEEE TRANSACTIONS ON EDUCATION, and was Chair of the CAS Nonlinear Circuits and Systems Technical Committee. He was the recipient of the Outstanding Master's Degree Candidate Award in 1989 and the Outstanding Ph.D. Degree Candidate Award in 1991, both from the UCLA School of Engineering and Applied Science. He is also the recipient of the Sigma Xi Prize for Outstanding Graduate Science Student at UCLA in 1991, the 1994 Guillemin-Cauer Award of the IEEE Circuits and Systems Society, the 1994 W. R. G. Baker Award of the IEEE, and a 1994 National Young Investigator Award from the National Science Foundation.